Training One Model to Master Cross-Level Agentic Actions via Reinforcement Learning

Kaichen He[1], Zihao Wang[1], Muyao Li[1], Anji Liu[2] and Yitao Liang[1]

[1]Peking University, [2]National University of Singapore, All authors are affiliated with Team CraftJarvis

The paradigm of agentic AI is shifting from engineered complex workflows to post-training native models. However, existing agents are typically confined to static, predefined action spaces—such as exclusively using APIs, GUI events, or robotic commands. This rigidity limits their adaptability in dynamic environments where the optimal granularity of interaction varies contextually. To bridge this gap, we propose CrossAgent, a unified agentic model that masters heterogeneous action spaces and autonomously selects the most effective interface for each step of a trajectory. We introduce a comprehensive training pipeline that integrates cold-start supervised fine-tuning with a Multi-Turn Group Relative Policy Optimization (GRPO) algorithm. This approach enables the agent to learn adaptive action switching—balancing high-level efficiency with low-level precision—without human-specified rules. Extensive experiments on over 800 tasks in the open-world Minecraft environment demonstrate that CrossAgent achieves state-of-the-art performance. By dynamically leveraging the strengths of diverse action spaces, our model significantly outperforms fixed-action baselines, exhibiting superior generalization and efficiency in long-horizon reasoning. All code and models are available at https://github.com/CraftJarvis/OpenHA.

1. Introduction

The field of agentic AI is undergoing a paradigm shift, moving from engineering complex workflows around pre-trained Large Language Models (LLMs) (Anthropic, 2025; OpenAI, 2023; Touvron et al., 2023; Yang et al., 2025) or Vision-Language Models (VLMs) (Achiam et al., 2023; Guo et al., 2025a; Team et al., 2023; Wang et al., 2024a) toward developing native agentic models through post-training. Contemporary native agents are typically characterized by the specific action spaces they master: GUI agents interact via mouse and keyboard events (openai, 2025; Qin et al., 2025), Deep Research agents utilize API calls (Huang et al., 2025; OpenAI, 2025b), Tool-Calling agents integrate with Model Context Protocol (MCP) services (Feng et al., 2025), and Vision-Language-Action (VLA) models execute embodied robotic commands (Belkhale et al., 2024b; Brohan et al., 2022, 2023b). However, prior research typically necessitated distinct action space designs for different tasks, often requiring manual selection and definition. To enable interaction within these spaces, researchers had to design specific action translation methods—such

as implementing MCP servers (Anthropic, 2024) for function calls or training learning-based policies for embodied control (Belkhale et al., 2024a).

However, relying on statically defined action spaces presents two fundamental challenges. First, specific action policies or translation layers are often brittle; for instance, an API-based `read_url` function may be blocked by CAPTCHA verifications, or a robotic policy may fail to execute a command with perfect precision, thereby capping the agent's success rate (Belkhale et al., 2024a; Driess et al., 2023). Second, the manual assignment of action spaces to tasks restricts the agent's flexibility, preventing it from effectively handling complex scenarios that require multimodal interactions. Recent works have begun to address this by bridging disjoint spaces to enhance generalization (Team, 2025). Specific approaches include integrating GUI and API-based actions into unified models (OpenAI, 2025a) or merging heterogeneous trajectories during training.

Crucially, we observe that the optimal action space often varies not only across tasks but also within a single task at the step level. Consider a
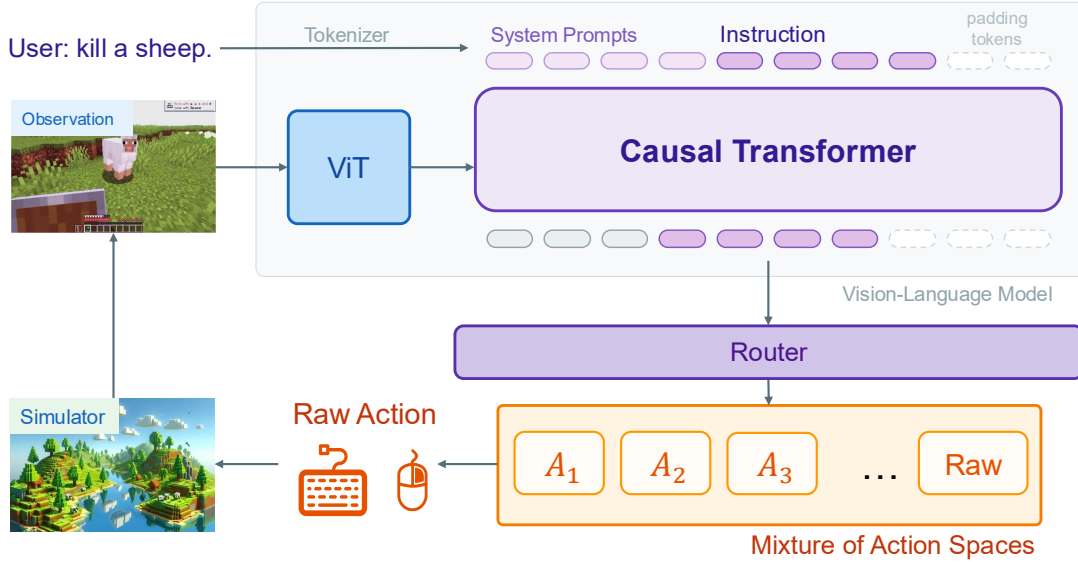
Figure 1 | **The CrossAgent Framework**. Unlike prior methods that confine the agent to a fixed action space (e.g., atomic movements) throughout a trajectory, CrossAgent dynamically switches across different action spaces to adapt to the context.

Deep Research agent: while the majority of information gathering is efficiently handled via search APIs, navigating a specific CAPTCHA-protected webpage may require precise GUI-level manipulation (OpenAI, 2025b). Consequently, a truly generalist agent must possess the ability to dynamically switch between action spaces, ranging from high-level APIs to low-level primitives, to maximize both success rates and efficiency.

To address these limitations, we introduce **CrossAgent**, a native agentic model trained to master multiple heterogeneous action spaces. Unlike traditional approaches that rely on static, human-specified rules, CrossAgent autonomously selects the most appropriate action space for each step of a trajectory. We propose a comprehensive training pipeline comprising three stages: cold-start supervised fine-tuning, Single-Turn Reinforcement Learning (RL), and Multi-Turn RL. By leveraging a Multi-Step Group Relative Policy Optimization (GRPO) (Guo et al., 2025b; Shao et al., 2024) algorithm, the agent learns to optimize its choices at the step level without explicit human intervention. This capability enables the agent to balance trade-offs dynamically; for example, prioritizing high-level actions for efficiency when applicable, while employing fine-grained atomic actions for precise control when necessary.

We validate our approach in the open-world Minecraft environment (Fan et al., 2022) (see Appendix A for environment details). Experimental results demonstrate that CrossAgent, despite being trained on only 30 tasks, successfully generalizes to over 800 tasks (Lin et al., 2023). It autonomously selects optimal action spaces, significantly outperforming baselines confined to fixed action spaces. Furthermore, the agent exhibits emergent behavior by optimizing not only for task success but also for trajectory efficiency, demonstrating robust capabilities for long-horizon reasoning.

Our main contributions are summarized as follows: 1) We propose CrossAgent, a unified agentic model capable of mastering heterogeneous action spaces and autonomously selecting the context-appropriate interface without relying on human-defined heuristics. 2) We introduce a comprehensive RL training pipeline utilizing Multi-Turn GRPO, enabling the agent to learn adaptive action switching within a single trajectory to maximize both task success and execution efficiency. 3) We achieve state-of-the-art performance on over 800 tasks in the Minecraft environment, demonstrating that adaptive action-space selection yields superior generalization and robustness compared to static baselines.

2. Related Works

2.1. Agentic Models with Different Actions

The deployment of VLM and LLM-based agents has expanded rapidly across various domains, ranging from physical environments to digital workspaces, each necessitating distinct interaction paradigms. In embodied settings, approaches such as OpenX (O'Neill et al., 2023), RT-H (Belkhale et al., 2024b), and OpenVLA (Kim et al., 2024) focus on mapping high-level instructions directly to physical control policies, effectively grounding language into continuous robot trajectories or joint angles (Brohan et al., 2023a; Driess et al., 2023). Transitioning to the digital domain, research on GUI and Web agents, such as Mind2Web and OS-World, centers on visual grounding, where agents learn to manipulate specific UI elements or generate low-level mouse and keyboard events to navigate dynamic screens (Deng et al., 2023; Li et al., 2025a; Team, 2025; Xu et al., 2024). In parallel, for logic-intensive tasks such as software engineering, agents like Claude and SWE-agent operate within discrete symbolic spaces, leveraging shell commands or standardized protocols like MCP to seamlessly integrate with external tools and APIs (Anthropic, 2024, 2025; Feng et al., 2025; Wang et al., 2024d; Yang et al., 2024). Similarly, many VLM-based game agents interact with video games directly via mouse and keyboard commands (Li et al., 2025b; Wang et al., 2025a,b).

2.2. Generalist Agent with Multi-Action Space

The static design of action spaces creates limitations when facing dynamic environments (Wang et al., 2025a). A common solution is to leverage the powerful in-context learning capabilities of foundation models (Anthropic, 2025; OpenAI, 2023; Team et al., 2023) to orchestrate workflows that specify transitions between action spaces for specific scenarios. For example, some computer-use agents (openai, 2025; Song et al., 2025) integrate tool usage (OpenAI, 2025b) with GUI actions to perform complex tasks: utilizing GUI actions for frontend interface validation while employing MCP when information retrieval is required. However, this approach often necessitates the design of complex, brittle pipelines.

A more unified approach involves fine-tuning agents across multiple action spaces to create a single generalist model. Prior explorations have demonstrated promising results in various domains, such as embodied agents (Bu et al., 2025; Lin et al., 2025), game agents (Wang et al., 2024b, 2025a,b), and computer use (Team, 2025). Experiments have demonstrated (Jia et al., 2025; Yan et al., 2025) that agents mastering distinct action spaces exhibit strong generalization capabilities and enhanced performance within specific domains.

However, previous efforts have often overlooked the potential of learning from experience to optimize these transitions. Our approach builds on prior work by advancing this paradigm, leveraging reinforcement learning to enable the model to autonomously adapt to the most appropriate action space at any given step.

3. Method

In this section, we introduce our approach for building an agent capable of autonomously selecting the most appropriate action space based on the task context.

We first formulate the problem. Consider an embodied control task modeled as a Markov Decision Process (MDP) with a state space $\mathcal{S}$ and a **composite** action space:

$$\mathcal{A} = \bigcup_{x=1}^{N} \mathcal{A}_x.$$

Each subspace $\mathcal{A}_x$ corresponds to a distinct class of actions, ranging from low-level motor controls to high-level motion primitives. Each subspace is associated with a specific interface or controller C_x that executes the abstract action $a_t \in \mathcal{A}_x$ within the environment.

At each timestep, the agent must determine **both** the optimal action space and the specific action content, balancing the immediate reward with execution efficiency. This leads to the follow-
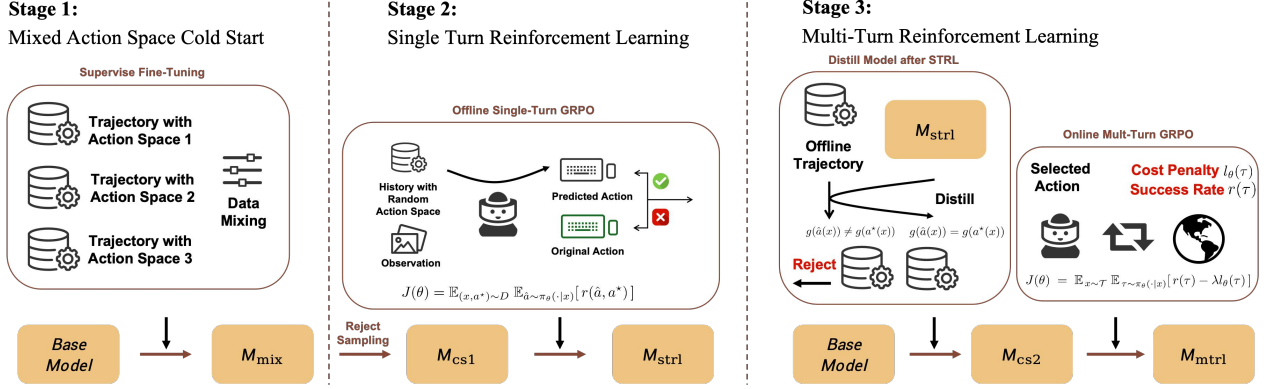
Figure 2 | **Overview of the CrossAgent Training Pipeline.** The pipeline comprises three distinct stages: Cold-Start Supervised Fine-Tuning (SFT), Single-Turn Reinforcement Learning (STRL), and Multi-Turn Reinforcement Learning (MTRL). In the first stage, the model learns to decode actions from a heterogeneous action space using a balanced dataset. During STRL, the model is fine-tuned to autonomously select the appropriate action space based on the immediate task context. Finally, in the MTRL stage, the policy is further optimized to balance task success rate with execution efficiency over long horizons. This progressive pipeline ensures CrossAgent effectively adapts its action granularity across a wide range of tasks.

ing objective:

$$ J = \mathbb{E} \left[\sum_t \left(r_t - \lambda_x \, \mathrm{cost}(a_t) \right) \right], $$

where the term $\lambda_x \, \mathrm{cost}(a_t)$ penalizes the computational or operational cost associated with different action granularities (e.g., token length or execution time).

The central challenge lies in the fact that different tasks, and even different phases within the same task, naturally favor different action spaces. Naive training on a unified space often fails to develop reliable, context-aware selection behavior. To address this, we introduce a phased training curriculum that progressively builds this capability. Beginning with supervised initialization, proceeding to strengthen local preferences through single-turn optimization, and culminating in long-horizon reasoning via multi-turn reinforcement learning, our framework equips the model with robust, dynamic action-space selection capabilities.

The overall training pipeline is illustrated in Figure 2. We detail each stage in the following subsections.

3.1. Stage-1: Mixed-Space SFT

In the initial stage, we establish the model's foundational capability to execute actions across heterogeneous spaces. We employ Supervised Fine-Tuning (SFT) on a balanced dataset comprising trajectories drawn from multiple action subspaces. By unifying data from these diverse modalities, the model learns to decode and generate valid actions within a composite action space. The primary objective of this stage is to construct a robust base model capable of grounding instructions into executable actions from diverse sources, prior to introducing complex decision-making tasks.

It is important to note that the resulting model, denoted as M_{mix}, does not yet autonomously select the optimal action space. Instead, it focuses on learning the syntax and semantics of multiple action types from the mixed data representation. The key challenge addressed here is enabling the model to interpret and generate actions for different spaces without modal interference, thereby laying a solid foundation for the adaptive decision-making mechanisms introduced in subsequent stages.

3.2. Stage-2: Single-Turn RL

In this stage, we empower the model to autonomously select the most appropriate action

space using **Single-Turn Reinforcement Learning (STRL)**.

Warm-up: Diversity-Enhanced SFT. Standard datasets typically lack explicit annotations indicating which action space is optimal for a given context. To bridge this gap, we first perform a warm-up phase to expose the model to multiple viable paths. We construct prompts that encourage the model to generate candidate actions across all available action spaces. These candidates are filtered via a **rejection sampling** approach: only actions that successfully execute the task (verified by the environment or a parser) are retained as ground-truth annotations. We then fine-tune the model on this rebalanced, multi-space dataset. The resulting model, denoted as M_{cs1}, acquires the capability to generate valid actions in various formats. However, empirical observation reveals that while M_{cs1} can operate across spaces, its selection strategy remains stochastic rather than strategic—it does not yet deliberately optimize the interface choice for task efficiency or robustness.

Optimization via GRPO. To transition from stochastic capability to strategic selection, we employ Group Relative Policy Optimization (GRPO) Shao et al. (2024), a reinforcement learning algorithm distinguished by its stability and resource efficiency. Unlike traditional methods like PPO that rely on a separate value function network for advantage estimation, GRPO utilizes the group statistics of multiple sampled outputs to estimate the baseline, thereby simplifying the optimization process.

Formally, for each query q, a group of outputs $\{o_1, o_2, \ldots, o_G\}$ is sampled from the current policy π_{old}. The policy π_θ is then optimized via the following objective:

$$
\begin{aligned}
J_{\text{GRPO}}(\theta) =& \mathbb{E}_{q \sim P(Q), \{o_i\}_{i=1}^{G} \sim \pi_{\text{old}}} \left[\frac{1}{G} \sum_{i=1}^{G} \frac{1}{|o_i|} \sum_{t=1}^{|o_i|} \right. \\
& \min \left(\rho_{i,t} \hat{A}_{i,t}, \text{clip} \left(\rho_{i,t}, 1 - \epsilon, 1 + \epsilon \right) \hat{A}_{i,t} \right) \\
& \left. - \beta D_{\text{KL}} [\pi_\theta || \pi_{\text{ref}}] \right]
\end{aligned}
\tag{1}
$$

where $\rho_{i,t} = \frac{\pi_\theta(o_i | q, o_{<t})}{\pi_{\text{old}}(o_i | q, o_{<t})}$ is the probability ratio.

Crucially, $\hat{A}_{i,t}$ represents the advantage estimate, which is calculated based on the relative performance of output o_i compared to the group mean, rather than a learned value function. This encourages the model to favor actions that outperform their peers within the same sampled group.

Since this stage focuses on immediate, one-step decision-making (viewing the task as a single-turn problem to optimize action space selection), we term it the STRL stage. To endow the cold-start model M_{cs1} with **action-space autonomy**, we cast each example in the dataset D as a one-step decision problem. Let $\{\mathcal{A}_k\}_{k=1}^{K}$ denote the set of string-level action spaces and $\mathcal{A} = \bigcup_k \mathcal{A}_k$. We utilize a deterministic parser $g : \mathcal{A} \rightarrow \mathcal{R}$ that maps an action string to its canonical raw representation in $\mathcal{R}$. The reward function is defined as:

$$
r(\hat{a}, a^\star) = \mathbb{1} \left\{ g(\hat{a}) = g(a^\star) \right\},
\tag{2}
$$

This reward is **action-space agnostic**: credit is granted whenever the parsed raw action matches the ground truth, regardless of the surface form (action space) used to generate $\hat{a}$. The STRL objective is to maximize the expected reward:

$$
J(\theta) = \mathbb{E}_{(x,a^\star) \sim D} \, \mathbb{E}_{\hat{a} \sim \pi_\theta(\cdot | x)} \left[r(\hat{a}, a^\star) \right].
\tag{3}
$$

Through this process, the model learns to ignore prior biases and autonomously select whichever action space most reliably yields the correct raw action for a given input. We denote the resulting model as M_{strl}.

3.3. Stage-3: Multi-Turn RL

Although M_{strl} achieves high accuracy in single-step action prediction, its probability distribution tends to be excessively peaked around specific action spaces, which limits exploration and hinders long-horizon task success. To explicitly cultivate robust, trajectory-level action-space selection, we adopt **Multi-Turn Reinforcement Learning (MTRL)**. In this stage, the optimization signal is derived from the episodic success rate, guiding the model to refine its policy for maximizing overall task completion rather than just immediate correctness.

Initialization via Self-Training (M_{cs2}). To accelerate training, we first distill the action-space

preferences of M_{strl} back into a supervised format. We perform inference over the initial dataset D using M_{strl}. For each example $(x, a^\star)$, let $\hat{a}$ denote the model's prediction and let $g(\cdot)$ map an action string to its canonical raw representation. We construct a relabeled dataset D_{strl} via the following rule:

$$a'(x) = \begin{cases} \hat{a}(x), & \text{if } g(\hat{a}(x)) = g(a^\star(x)), \\ a^\star(x), & \text{otherwise.} \end{cases} \quad (4)$$

Essentially, if the predicted action is semantically consistent with the ground truth (as verified by g), we replace the original label with the action space chosen by M_{strl}; otherwise, we retain the original label. This relabeling preserves the raw-action semantics while aligning the surface-level action space with the model's learned preferences. We then fine-tune the base model on this relabeled dataset D_{strl}, following the same protocol as the previous SFT stage. We denote the resulting model as M_{cs2}. Since the ground truth in D_{strl} reflects the optimized choices of M_{strl}, M_{cs2} initializes the MTRL stage with a strong prior for appropriate action-space selection.

Trajectory Optimization. We subsequently fine-tune M_{cs2} using multi-turn RL on a curated task set $\mathcal{T}$. Given an instruction $x \in \mathcal{T}$, the policy $\pi_\theta(\cdot \mid x)$ interacts with the environment to generate a trajectory τ. We utilize a binary episodic reward:

$$r(\tau) = \mathbb{1}\{\text{success}(\tau)\} \quad (5)$$

The objective is to maximize the task success rate while penalizing excessive generation costs:

$$J(\theta) = \mathbb{E}_{x \sim \mathcal{T}} \, \mathbb{E}_{\tau \sim \pi_\theta(\cdot \mid x)} [\, r(\tau) - \lambda l_\theta(\tau) \,]. \quad (6)$$

where $l_\theta(\tau)$ denotes the total number of tokens produced by the model throughout the trajectory. This penalty term encourages the model to prefer concise action spaces (e.g., high-level APIs) over verbose ones (e.g., raw primitive commands) when both yield success. A detailed discussion of the specific GRPO implementation for this stage is provided in Appendix C.

By optimizing Equation 6, the model improves its capacity for dynamic, context-aware action space adaptation over long horizons. We denote the final model as M_{mtrl}, which serves as our final **CrossAgent**.

4. Experiments

In this section, we present a comprehensive experimental evaluation to empirically validate our proposed framework. We specifically investigate how the capacity to dynamically utilize heterogeneous action spaces influences the performance of general-purpose agents in open-ended environments. We begin by detailing our experimental setup, including model training protocols, the large-scale benchmark used for evaluation, and the specific metrics employed. Our analysis is structured around three core research questions:

Q1: Action Space Sensitivity. How does the choice of a fixed action space impact model performance, and does the optimal action space vary across different task categories?

Q2: Benefits of Dynamic Switching. Does the ability to autonomously and dynamically select the most appropriate action space yield superior performance compared to static baselines?

Q3: Generalization and Robustness. Does the model maintain its generalization capabilities on unseen tasks after being fine-tuned via multi-turn RL on a limited set of training tasks?

4.1. Experimental Setup

Benchmark. We utilize Minecraft (version 1.16.5) as our primary evaluation environment (Guss et al., 2019). The agent's observation space consists exclusively of first-person RGB images with a resolution of $360 \times 640 \times 3$. The action space employs a discrete, human-like interface, comprising mouse movements, clicks, and keyboard commands. Further details regarding the observation and action spaces are provided in Appendix A.

To assess our agent, we employ the OpenHA benchmark suite (Wang et al., 2025a), which features over 800 tasks. All tasks are manually designed and verified, ensuring both richness and feasibility. We categorize these tasks into three groups based on the primary skills required: 1) **Mine Blocks**: Tasks involving navigation and physical interaction within the environment (e.g., locating and chopping down a specific type of

Table 1 | The evaluation results of Minecraft agents across more than 800 tasks are presented.For each task category, we report three metrics: the success rate of a representative task (indicated by its icon), the percentage of tasks that the agent succeeds at least once (FT), and the average success rate across all tasks in the category (ASR) with standard deviation. Results highlighted in blue correspond to the second-best performances, while those in red represent the state-of-the-art performance for each metric across all agents.

Method	Mine Blocks			Kill Entities			Craft Items			All Tasks	
	🟫	FT ↑	ASR ↑	🟥	FT ↑	ASR ↑	↗	FT ↑	ASR ↑	FT ↑	ASR ↑
Instruction-Conditioned Policies											
VPT (Baker et al., 2022)	20.0	30.7	$6.0^{\pm 11.4}$	10.0	24.6	$3.6^{\pm 7.7}$	0.0	6.7	$0.8^{\pm 3.3}$	20.7	$3.5^{\pm 8.4}$
STEVE-I (Lifshitz et al., 2024)	50.0	29.4	$8.0^{\pm 17.0}$	0.0	14.7	$3.9^{\pm 12.0}$	0.0	16.4	$3.2^{\pm 8.4}$	20.2	$5.0^{\pm 12.4}$
ROCKET-1 (Cai et al., 2024)	60.0	57.5	$18.9^{\pm 24.3}$	60.0	63.9	$27.9^{\pm 29.3}$	0.0	0.0	$0.0^{\pm 0.0}$	45.5	$15.6^{\pm 24.9}$
JARVIS-VLA (Li et al., 2025b)	55.0	55.3	$30.0^{\pm 35.4}$	60.0	61.9	$18.5^{\pm 22.7}$	40.0	74.3	$25.1^{\pm 23.9}$	63.8	$24.5^{\pm 28.4}$
VLM-based Agents											
TextHA (Wang et al., 2025a)	60.0	36.3	$27.2^{\pm 38.2}$	0.0	19.2	$8.7^{\pm 23.7}$	50.0	43.9	$26.0^{\pm 35.2}$	33.1	$20.6^{\pm 34.0}$
GroundingHA (Cai et al., 2024)	90.0	61.0	$37.1^{\pm 38.5}$	50.0	90.1	$26.5^{\pm 23.4}$	15.0	27.5	$6.7^{\pm 10.8}$	59.5	$23.4^{\pm 29.6}$
UI-TARS-1.5 (Seed, 2025)	-	-	$42.1^{\pm 20.4}$	-	-	$31.0^{\pm 16.4}$	0	0	$36.7^{\pm 17.2}$	-	33.8
MotionHA (Belkhale et al., 2024b)	70.0	51.0	$27.4^{\pm 35.2}$	20.0	29.5	$4.3^{\pm 10.8}$	0.0	0.0	$0.0^{\pm 0.0}$	29.8	$10.6^{\pm 24.4}$
LanguageHA (Driess et al., 2023)	60.0	31.3	$11.3^{\pm 14.5}$	0.0	12.8	$6.5^{\pm 9.3}$	5.0	19.3	$6.3^{\pm 9.2}$	21.1	$8.0^{\pm 11.5}$
LatentHA (Wang et al., 2024c)	70.0	54.2	$24.4^{\pm 31.1}$	50.0	24.6	$8.5^{\pm 17.9}$	0.0	19.1	$3.0^{\pm 7.5}$	32.6	$12.0^{\pm 23.0}$
OpenHA (Wang et al., 2025a)	80.0	67.3	$30.1^{\pm 13.9}$	70.0	62.6	$32.5^{\pm 9.2}$	80.0	58.8	$31.9^{\pm 13.7}$	62.8	$31.5^{\pm 12.5}$
Game-TARS (Wang et al., 2025b)	-	-	$50.14^{\pm 20.7}$	-	-	$38.1^{\pm 24.6}$	-	-	$39.1^{\pm 27.5}$	-	42.2
Ours											
CrossAgent(w/o STRL stage)	63.6	35.1	$39.0^{\pm 46.5}$	28.6	43.9	$27.7^{\pm 43.9}$	57.1	55.7	$58.0^{\pm 48.4}$	44.9	$41.6^{\pm 47.9}$
CrossAgent	94.7	45.2	$40.0^{\pm 48.3}$	66.6	58.1	$45.1^{\pm 43.5}$	83.3	72.7	$78.8^{\pm 41.0}$	58.7	$54.6^{\pm 47.6}$

tree); 2) **Craft Items**: Tasks requiring complex interactions with graphical user interfaces (GUIs), such as crafting at a table or smelting ores in a furnace; 3) **Kill Entities**: Tasks focusing on survival and combat, requiring the agent to engage with dynamic mobs.

In our evaluation protocol, we adopt two primary metrics: **Finished Tasks (FT)** and **Average Success Rate (ASR)**. FT measures the proportion of distinct tasks within a category for which the agent achieves at least one successful completion, reflecting the agent's *task coverage* and generalization range. ASR quantifies the mean success rate across all tasks in the category, capturing *reliability* by accounting for the consistency of the agent's performance on each specific task.

Training Setup. 1) **Model Initialization**. We initialize our training with Qwen2-VL-7B-Instruct (Wang et al., 2024a), a pre-trained vision-language model demonstrating strong multimodal understanding. We fine-tune this model using diverse Minecraft-specific VQA and cap-

tioning datasets (Li et al., 2025b), yielding the base model M_{base}. 2) **Dataset Construction**. We generate grounding and motion ground-truth annotations by integrating two systems: a SAM-based (Ravi et al., 2024) grounding pipeline and a motion-generation module built upon a fine-tuned MineCLIP (Fan et al., 2022) model. These systems annotate both VPT data and a subset of contractor-collected trajectories. Since suitable grounding or motion annotations cannot be generated for every trajectory, the resulting action space distribution is imbalanced. These annotated data are integrated to form the mixed-action-space dataset D_{mix}.

We then process M_{base} and D_{mix} through the pipeline described in section 3. During the MTRL stage, we select 10 tasks from each of the three primary OpenHA categories: `craft_item`, `kill_entity`, and `mine_block`. This results in a total of 30 training tasks. For online RL, we train using GRPO for over 80 iterations, with each iteration involving over 6,400 environment interactions. This extensive training regime allows

the model's performance to converge to a stable, high-level policy.

Baselines. Our analysis compares CrossAgent against variants of the base model M_{base} fine-tuned (via either SFT or RL) on datasets restricted to single-type action spaces. We categorize these baselines based on their action space formats: **LanguageHA**, **GroundingHA**, **MotionHA**, **RawHA**, and **LatentHA**. We also include several representative LLM-based agents, such as Jarvis-VLA (Li et al., 2025b), and hierarchical agents fine-tuned with SFT on fixed action spaces. For broader context, we further compare against specialized policies trained on the VPT dataset, including the original VPT (Baker et al., 2022), ROCKET-1 (Cai et al., 2024), and STEVE-1 (Lifshitz et al., 2024).

4.2. Main Results

As presented in Table 1, CrossAgent achieves state-of-the-art performance across all three major task categories. It substantially outperforms existing instruction-conditioned policies and hierarchical agents on overall evaluation metrics. Our analysis highlights three key observations:

Clear Advantages Over Single-Action-Space Agents. Agents confined to a single action space exhibit strong but narrow specialization, leading to pronounced performance asymmetries across task types. For instance, **GroundingHA** excels at *Kill Entity* tasks (FT: 90.1%), where visual tracking and sustained attention are essential. Conversely, **MotionHA** performs better on *Mine Block* tasks that emphasize locomotion, while **RawHA** demonstrates advantages in *Craft Item* tasks due to its fine-grained control capabilities. However, these advantages are domain-specific and fail to generalize across categories—none of the single-action-space baselines achieve uniformly strong results. This underscores the inherent limitations of rigid, action-space-specific designs.

RL Facilitates Robust OOD Generalization. Comparing SFT-only agents (e.g., OpenHA, MotionHA) with their RL-enhanced counterparts (e.g., CrossAgent variants) reveals consistent and substantial gains in both ASR and FT. Remarkably, although RL fine-tuning is conducted on only
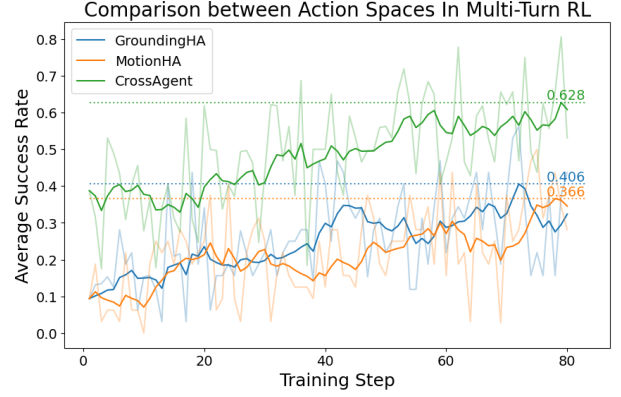

Figure 3 | **Performance Comparison Across Action Spaces.** The heterogeneous action space of CrossAgent enables superior data efficiency and higher asymptotic performance during multi-turn reinforcement learning, compared to single-space baselines.

30 tasks, the improvements generalize effectively to over 800 evaluation tasks, many of which differ significantly from the training distribution. These gains are particularly pronounced in fine-grained control domains such as *Craft Item*, where trajectory optimization offers a distinct advantage. This confirms that reinforcement learning, when applied atop large pre-trained VLA models, serves as a critical component for achieving out-of-distribution (OOD) generalization in scalable embodied agents.

CrossAgent Achieves Balanced, Omni-Category Performance. Unlike prior hierarchical or modular agents, CrossAgent achieves the best or second-best results in nearly every metric across all categories. It demonstrates a unique ability to balance proficiency across *Mine Blocks*, *Kill Entities*, and *Craft Items*—a versatility not observed in prior baselines. Furthermore, it attains high peak success rates (e.g., 94.7% in Mine Blocks, 83.3% in Craft Items) without sacrificing generality. These results strongly suggest that CrossAgent effectively learns to coordinate and select the most suitable action space based on task context, rather than over-specializing in a single mode. This dynamic switching mechanism is key to its robust performance.

4.3. Ablation Studies

Impact of Mixed Action Spaces. To validate the advantages of operating within a unified, hetero-
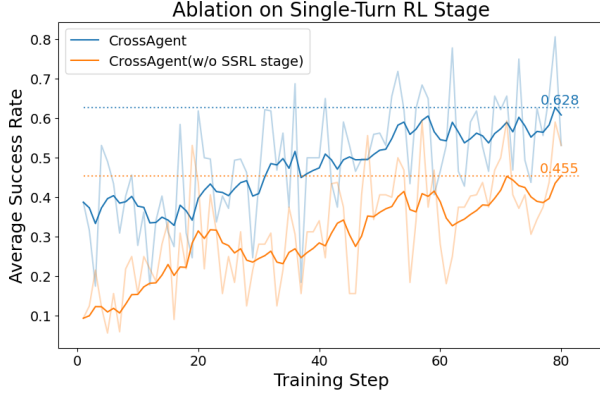
Figure 4 | **Effect of the Single-Turn RL (STRL) Stage.** Training curves comparing CrossAgent with and without the STRL phase. The inclusion of STRL significantly enhances training efficiency and accelerates convergence in the subsequent MTRL stage, despite its low computational cost.

geneous action space compared to single-space constraints, we conducted an ablation study on the action space itself. We constructed single-space baselines (GroundingHA and MotionHA) by modifying the initialization of the Multi-Turn RL (MTRL) stage. Specifically, instead of cold-starting the model M_{cs2} with the full mixed dataset D_{strl}, we fine-tuned the base model using only the grounding-space subset or the motion-space subset of D_{strl}, respectively. All models, including CrossAgent, underwent identical SFT cold-start training for 200 steps prior to MTRL. The scale of our dataset ensured that no samples were repeated during this phase.

We monitored the task success rates throughout the MTRL training process, as illustrated in Figure 3. CrossAgent demonstrates significantly faster convergence and higher asymptotic performance compared to the single-space baselines. This indicates that the capacity to autonomously and dynamically select among multiple action spaces affords the model greater flexibility. When confronting diverse and complex task dynamics, this flexibility translates into higher success rates and more robust task completion, thereby significantly enhancing the data efficiency of online reinforcement learning.

Necessity of the STRL Stage. We further investigate the contribution of the Single-Turn RL (STRL) phase to the overall pipeline. To construct a variant *without* STRL, we bypass Stage 2 entirely. Instead of using the STRL-relabeled dataset D_{strl} to initialize the MTRL stage, we employ the original balanced dataset D_{bal} (from Stage 1) for the cold-start process. We then perform identical MTRL training on both the standard CrossAgent and this ablation variant.

As shown in Figure 4, the training curves reveal substantial improvements in both sample efficiency and final performance when STRL is included. This suggests that the STRL phase, despite its relatively low computational cost, effectively warms up the model's policy for action-space selection. This initialization proves critical, as it enables more efficient exploration and reliable action sequencing during the computationally expensive MTRL stage. Quantitative results in Table 1 further confirm that the STRL-enhanced CrossAgent achieves consistently higher success rates across a wider range of tasks, demonstrating superior cross-task generalization.

4.4. Generalization Evaluation

While the results in Table 1 demonstrate the impressive OOD performance of CrossAgent, a critical question remains regarding the trade-off between reinforcement learning and generalization. RL methods are often prone to overfitting the training distribution. To investigate this rigorously, we compare the agent's performance on In-Distribution (ID) training tasks versus OOD evaluation tasks, as detailed in Table 2.

Robust Performance on OOD Tasks. CrossAgent achieves the highest success rate in *Craft Items* (78.8%) and demonstrates strong overall performance in *Mine Blocks* (40.0%) and across *All Tasks* (49.1%). These results indicate that CrossAgent possesses superior generalization capabilities compared to other RL baselines. Notably, the ablation variant **CrossAgent (w/o STRL)** shows consistent performance but trails the full version, particularly in *Craft Items* (58.0% vs. 78.8%) and *All Tasks* (39.7% vs. 49.1%). This significant gap confirms that the STRL stage is instrumental in preventing the policy from collapsing into sub-optimal modes, thereby facilitating better generalization. In contrast, single-

Table 2 | Evaluation results of RL agents on In-Distribution (ID) and Out-of-Distribution (OOD) tasks. We report the success rate and standard deviation. **Red** indicates the best performance, and **Blue** indicates the second best.

Method	In-Distribution Evaluation				Out-of-Distribution Evaluation			
	Mine Blocks	Kill Entities	Craft Items	All Tasks	Mine Blocks	Kill Entities	Craft Items	All Tasks
RawHA-RL	$65.2^{\pm32.1}$	$41.6^{\pm21.8}$	$96.2^{\pm3.8}$	$70.1^{\pm33.6}$	$28.9^{\pm44.2}$	$28.4^{\pm32.3}$	$69.8^{\pm44.4}$	$42.4^{\pm45.1}$
GroundingHA-RL	$46.8^{\pm35.6}$	$48.8^{\pm34.5}$	$69.3^{\pm28.4}$	$52.6^{\pm31.5}$	$27.2^{\pm42.4}$	$33.9^{\pm35.9}$	$57.2^{\pm48.1}$	$39.4^{\pm44.3}$
MotionHA-RL	$78.6^{\pm24.6}$	$44.0^{\pm25.2}$	$63.0^{\pm20.7}$	$61.9^{\pm27.5}$	$41.5^{\pm45.5}$	$26.8^{\pm26.7}$	$49.0^{\pm47.3}$	$39.1^{\pm42.0}$
CrossAgent(w/o STRL)	$63.3^{\pm28.9}$	$24.0^{\pm26.4}$	$76.1^{\pm27.2}$	$54.5^{\pm35.3}$	$39.0^{\pm46.5}$	$22.2^{\pm42.6}$	$58.0^{\pm48.4}$	$39.7^{\pm48.1}$
CrossAgent	$70.7^{\pm33.3}$	$52.1^{\pm22.9}$	$83.7^{\pm25.5}$	$68.8^{\pm30.5}$	$40.0^{\pm48.3}$	$28.4^{\pm33.2}$	$78.8^{\pm41.0}$	$49.1^{\pm46.6}$

space agents like **RawHA-RL**, **GroundingHA-RL**, and **MotionHA-RL** exhibit significant variance. They struggle considerably with OOD tasks outside their specialized domains, suggesting that restricting the action space limits the model's ability to transfer learned skills to novel scenarios.

Analysis of the Generalization Gap (ID vs. OOD). Comparing ID and OOD performance reveals distinct behaviors: Baselines such as **RawHA-RL** and **MotionHA-RL** achieve very high success rates on ID tasks (e.g., 96.2% for RawHA-RL in Craft Items), reflecting a strong fit to their training environments. However, their sharp performance drop on OOD tasks highlights a tendency toward overfitting. **CrossAgent**, while also performing strongly on ID tasks (83.7% in Craft Items, 68.8% overall), maintains a much narrower generalization gap. This indicates that while RL inevitably introduces some degree of specialization to the training set, CrossAgent's dynamic action-space selection mechanism mitigates catastrophic overfitting. It successfully translates the "general understanding" of environment dynamics learned during training into proficiency on unseen tasks.

Conclusion on RL Fine-Tuning. The results underscore a key insight: the benefits of RL fine-tuning, especially when combined with heterogeneous action spaces, far outweigh the risks of overfitting. CrossAgent sets a new standard for OOD generalization, establishing that a unified agent capable of dynamic interface switching is more robust than specialized experts. The combination of large-scale pretraining, the STRL warm-up, and MTRL optimization enables the agent to master complex distributions, proving that reinforcement learning is a viable path for building general-purpose open-world agents.
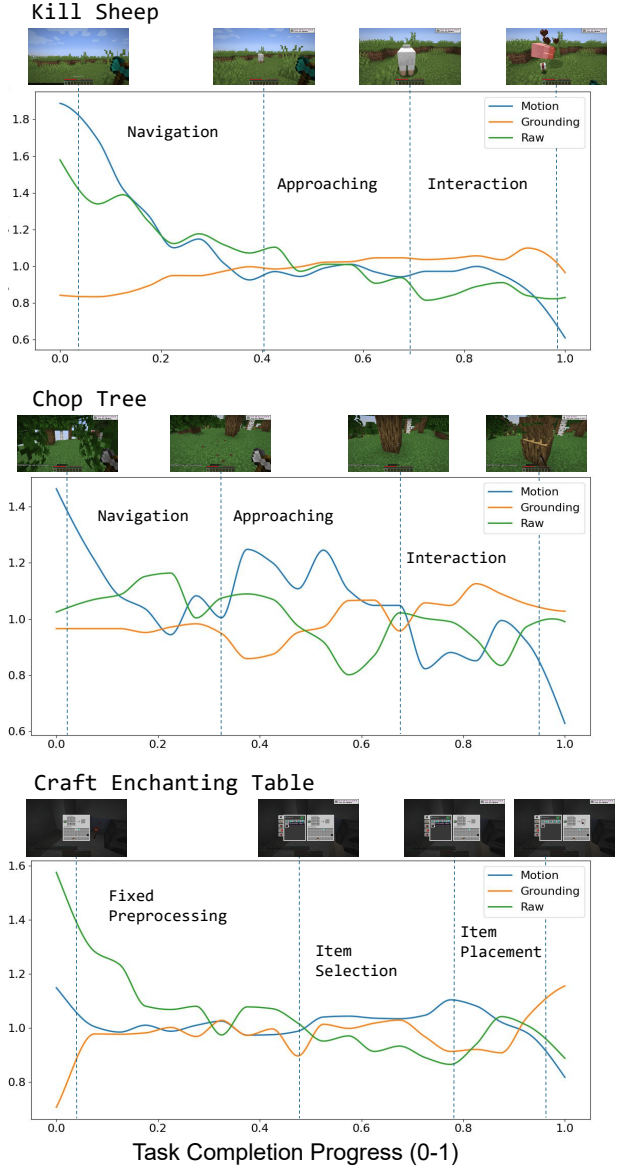

Figure 5 | **Case Study: Action distribution during the `Kill Sheep`, `Chop Tree` and `Craft Enchanting` task.** The density curves of each tasks, aggregated over 20 episodes, of different action spaces (Motion, Grounding, Raw) across different task phases. The dynamic shifts in distribution demonstrate the model's in-context adaptive strategy.

4.5. Case Studies

To qualitatively demonstrate the efficacy of dynamic action space selection, we analyze CrossAgent's behavior across three representative tasks: `Kill Sheep` (Kill Entities), `Chop Tree` (Mine Blocks), and `Craft Enchanting Table` (Craft Items). These cases illustrate how the agent adapts its interface strategy to meet the distinct demands of different task phases. Figure 6 illustrates the probability density curves of different action spaces selected by CrossAgent with respect to task completion progress.

Kill Sheep. As illustrated in the `Kill Sheep` task proceeds through three distinct stages: **1) Navigation**: Rotating the camera and traversing the terrain to locate a target. **2) Approaching**: Locking focus on the sheep and closing the distance. **3) Interaction**: Executing attacks to deal damage. During the **Navigation Stage**, CrossAgent predominantly employs the coarse yet efficient Motion Action Space to scan large areas rapidly. Once the sheep enters the field of view, the agent transitions to the **Approaching Stage**, characterized by a balanced mix of action spaces: Motion Actions facilitate fast movement, Grounding Actions provide continuous visual tracking cues, and Raw Actions enable fine-grained adjustments to navigate around obstacles. Finally, in the **Interaction Stage**, sustained Grounding Actions ensure precise targeting of the moving entity, while Raw Actions are leveraged to execute high-frequency attack commands efficiently. This progression demonstrates CrossAgent's ability to switch contextually: prioritizing search efficiency initially, then blending modalities for pursuit, and finally optimizing for targeting precision.

Chop Tree. The `Chop Tree` task shares the Navigation-Approaching-Interaction structure with `Kill Sheep` but exhibits distinct characteristics. Trees are static targets, and the agent typically spawns in forested areas where targets are abundant. Consequently, the task requires less precise tracking than hunting moving entities. Motion Actions dominate the navigation and approaching phases. Unlike the `Kill Sheep` task, where the agent must constantly adjust its bearing to chase a target, the static nature of trees allows the agent to rely heavily on the simple 'Walk Forward' primitive within the Motion Space. In the interaction phase, Grounding Actions are engaged to accurately target the specific wood block, ensuring successful harvesting.

Craft Enchanting Table. Crafting tasks involve complex, multi-step GUI interactions. We categorize the workflow into three phases: **1) Fixed Preprocess**: Opening the recipe book and toggling the 'Only Show Craftable Items' filter. Since these steps are invariant across tasks, Raw Actions dominate this phase, leveraging their precision and stability to execute rote "muscle memory" sequences efficiently. **2) Item Selection**: Locating and selecting the target item within the grid. Here, the identification capability of the Grounding Space becomes crucial for visually recognizing the correct icon. Simultaneously, the Motion Space aids in smooth cursor traversal. **3) Item Placement**: Retrieving the crafted item from the result slot. The Grounding Space is again pivotal, helping the model accurately coordinate the cursor between the result slot and the inventory, mitigating the risk of mis-clicks.

Figure 5 further illustrates some key frames and corresponding outputs from the CrossAgent rollout. These examples demonstrate CrossAgent's ability to adaptively select the suitable action space in context, leading to more precise and efficient task execution.

The qualitative rollouts corroborate our statistical findings, offering a concrete window into the agent's decision-making process. The generated trajectories reveal that CrossAgent's switching mechanism is semantically coherent rather than stochastic. For instance, the seamless transition from high-level *Motion* primitives for efficient exploration to precise *Grounding* or *Raw* commands for interaction closely mirrors human behavioral patterns. This qualitative evidence, combined with the quantitative performance metrics, strongly validates that CrossAgent has successfully internalized a hierarchical understanding of open-world tasks. It demonstrates that the model does not merely memorize trajectories but learns to autonomously decompose complex objectives into optimal sequences of heterogeneous actions, thereby achieving both robustness and efficiency.
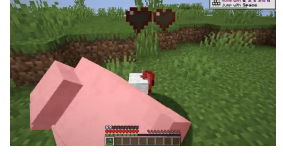
Kill Sheep

Motion:move forward	Grounding:Approach `<|object_ref_start|>`sheep `<|object_ref_end|>`(780,661)	Action: move(0, 0) and press() and click(left)"	Motion: no_op

Chop Tree

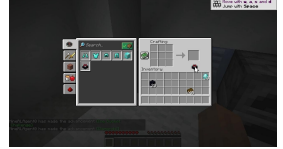|			
Action: move(-2, 4) and press() and click(left)	Grounding: Attack `<|object_ref_start|>`oak log`<|object_ref_end|>`<`|point_start|>`(938,581)`<|point_end|>`	Action: move(0, 0) and press(w) and click(left)"	Action: move(0, 0) and press(w) and click(left)

Craft Enchanting Table

Action: move(-16, -9) and press()	Motion: cursor move left and down	Grounding: move_camera `<|object_ref_start|>`enchanting_table`<|object_ref_end|>`<`|point_start|>`(338,464)`<|point_end|>`	Motion: cursor move down
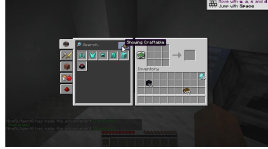
Figure 6 | **Example Rollouts of `Kill Sheep`, `Chop Tree` and `Craft Enchanting` task.** The prefixes 'Motion:', 'Grounding:', and 'Action:' denote actions from the Motion Space, Grounding Space, and Raw Space, respectively.

5. Conclusion

In this work, we address the fundamental limitations of contemporary agentic models restricted to static, predefined action spaces. We introduce **CrossAgent**, a native agentic model that unifies heterogeneous interaction capabilities—ranging from high-level scripts to low-level atomic commands—into a single policy. By leveraging a comprehensive training pipeline anchored by Single- and Multi-Turn Group Relative Policy Optimization (GRPO), CrossAgent learns to autonomously select the optimal action space at the step level, effectively balancing execution precision with trajectory efficiency. Extensive evaluations on over 800 Minecraft tasks demonstrate that this adaptive approach achieves state-of-the-art performance, substantially outperforming baselines confined to fixed action spaces. These results validate that treating action-space selection as a learnable component—rather than a static, hand-crafted constraint—significantly enhances both performance and generalization.

Nevertheless, we acknowledge certain avenues for future improvement. First, the Multi-Turn RL stage, while effective, entails non-negligible computational costs; future investigations into more sample-efficient or offline RL algorithms could significantly accelerate this process. Second, transferring capabilities learned in Minecraft to physical robotics introduces distinct challenges such as safety constraints and real-time feedback latency. Addressing these sim-to-real gaps represents a primary direction for our future work. Ultimately, the ability to dynamically switch between heterogeneous interfaces is a pivotal step toward building generalist agents in open-ended environments.

References

J. Achiam, S. Adler, S. Agarwal, L. Ahmad, I. Akkaya, F. L. Aleman, D. Almeida, J. Altenschmidt, S. Altman, S. Anadkat, et al. Gpt-4 technical report. arXiv preprint arXiv:2303.08774, 2023.

Anthropic. Introducing the model context protocol, 2024. URL https://www.anthropic.com/news/model-context-protocol.

Anthropic. Introducing claude 4, 2025. URL https://www.anthropic.com/news/claude-4.

B. Baker, I. Akkaya, P. Zhokov, J. Huizinga, J. Tang, A. Ecoffet, B. Houghton, R. Sampedro, and J. Clune. Video pretraining (vpt): Learning to act by watching unlabeled online videos. Advances in Neural Information Processing Systems, 35:24639–24654, 2022.

S. Belkhale, T. Ding, T. Xiao, P. Sermanet, Q. Vuong, J. Tompson, Y. Chebotar, D. Dwibedi, and D. Sadigh. Rt-h: Action hierarchies using language. arXiv preprint arXiv:2403.01823, 2024a.

S. Belkhale, T. Ding, T. Xiao, P. Sermanet, Q. Vuong, J. Tompson, Y. Chebotar, D. Dwibedi, and D. Sadigh. Rt-h: Action hierarchies using language. arXiv preprint arXiv:2403.01823, 2024b.

A. Brohan, N. Brown, J. Carbajal, Y. Chebotar, J. Dabis, C. Finn, K. Gopalakrishnan, K. Hausman, A. Herzog, J. Hsu, et al. Rt-1: Robotics transformer for real-world control at scale. arXiv preprint arXiv:2212.06817, 2022.

A. Brohan, N. Brown, J. Carbajal, Y. Chebotar, X. Chen, K. Choromanski, T. Ding, D. Driess, A. Dubey, C. Finn, et al. Rt-2: Vision-language-action models transfer web knowledge to robotic control. arXiv preprint arXiv:2307.15818, 2023a.

A. Brohan, N. Brown, J. Carbajal, Y. Chebotar, X. Chen, K. Choromanski, T. Ding, D. Driess, A. Dubey, C. Finn, et al. Rt-2: Vision-language-action models transfer web knowledge to robotic control. arXiv preprint arXiv:2307.15818, 2023b.

Q. Bu, Y. Yang, J. Cai, S. Gao, G. Ren, M. Yao, P. Luo, and H. Li. Univla: Learning to act anywhere with task-centric latent actions. arXiv preprint arXiv:2505.06111, May 2025.

S. Cai, Z. Wang, K. Lian, Z. Mu, X. Ma, A. Liu, and Y. Liang. Rocket-1: Mastering open-world interaction with visual-temporal context prompting. arXiv preprint arXiv:2410.17856, 2024.

J. Deng, Z. Wang, S. Cai, A. Liu, and Y. Liang. Open-world skill discovery from unsegmented demonstrations. arXiv preprint arXiv:2503.10684, 2025.

X. Deng, K. Guu, P. Pasupat, A. Akyürek, S. Zhuang, W. Chen, T. Hashimoto, K. Guu, and P. Liang. Mind2web: Towards a generalist agent for the web. In NeurIPS Datasets and Benchmarks, 2023. URL https://arxiv.org/abs/2306.06070.

D. Driess, F. Xia, M. S. Sajjadi, C. Lynch, A. Chowdhery, B. Ichter, A. Wahid, J. Tompson, Q. Vuong, T. Yu, et al. Palm-e: An embodied multimodal language model. arXiv preprint arXiv:2303.03378, 2023.

L. Fan, G. Wang, Y. Jiang, A. Mandlekar, Y. Yang, H. Zhu, A. Tang, D.-A. Huang, Y. Zhu, and A. Anandkumar. Minedojo: Building open-ended embodied agents with internet-scale knowledge. Advances in Neural Information Processing Systems Datasets and Benchmarks, 2022.

J. Feng, S. Huang, X. Qu, G. Zhang, Y. Qin, B. Zhong, C. Jiang, J. Chi, and W. Zhong. Retool: Reinforcement learning for strategic tool use in llms. arXiv preprint arXiv:2504.11536, 2025.

D. Guo, F. Wu, F. Zhu, F. Leng, G. Shi, H. Chen, H. Fan, J. Wang, J. Jiang, J. Wang, et al. Seed1. 5-vl technical report. arXiv preprint arXiv:2505.07062, 2025a.

D. Guo, D. Yang, H. Zhang, J. Song, R. Zhang, R. Xu, Q. Zhu, S. Ma, P. Wang, X. Bi, et al.

Deepseek-r1: Incentivizing reasoning capability in llms via reinforcement learning. arXiv preprint arXiv:2501.12948, 2025b.

W. H. Guss, B. Houghton, N. Topin, P. Wang, C. Codel, M. Veloso, and R. Salakhutdinov. Minerl: A large-scale dataset of minecraft demonstrations. arXiv preprint arXiv:1907.13440, 2019.

Y. Huang, Y. Chen, H. Zhang, K. Li, H. Zhou, M. Fang, L. Yang, X. Li, L. Shang, S. Xu, et al. Deep research agents: A systematic examination and roadmap. arXiv preprint arXiv:2506.18096, 2025.

H. Jia, J. Liao, X. Zhang, H. Xu, T. Xie, C. Jiang, M. Yan, S. Liu, W. Ye, and F. Huang. Osworld-mcp: Benchmarking mcp tool invocation in computer-use agents. arXiv preprint arXiv:2510.24563, Nov. 2025.

M. J. Kim, K. Pertsch, S. Karamcheti, T. Xiao, A. Balakrishna, S. Nair, R. Rafailov, E. Foster, G. Lam, P. Sanketi, et al. Openvla: An open-source vision-language-action model. arXiv preprint arXiv:2406.09246, 2024.

J. Lee, J. Duan, H. Fang, Y. Deng, S. Liu, B. Li, B. Fang, J. Zhang, Y. R. Wang, S. Lee, et al. Molmoact: Action reasoning models that can reason in space. arXiv preprint arXiv:2508.07917, 2025.

K. Li, Z. Meng, H. Lin, Z. Luo, Y. Tian, J. Ma, Z. Huang, and T.-S. Chua. Screenspot-pro: Gui grounding for professional high-resolution computer use. arXiv preprint arXiv:2504.07981, 2025a.

M. Li, Z. Wang, K. He, X. Ma, and Y. Liang. Jarvis-vla: Post-training large-scale vision language models to play visual games with keyboards and mouse. arXiv preprint arXiv:2503.16365, 2025b.

S. Lifshitz, K. Paster, H. Chan, J. Ba, and S. McIlraith. Steve-1: A generative model for text-to-behavior in minecraft. Advances in Neural Information Processing Systems, 36, 2024.

F. Lin, R. Nai, Y. Hu, J. You, J. Zhao, and Y. Gao. Onetwovla: A unified vision-language-action

model with adaptive reasoning. arXiv preprint arXiv:2505.11917, 2025.

H. Lin, Z. Wang, J. Ma, and Y. Liang. Mcu: A task-centric framework for open-ended agent evaluation in minecraft. arXiv preprint arXiv:2310.08367, 2023.

A. O'Neill, A. Rehman, A. Gupta, A. Maddukuri, A. Gupta, A. Padalkar, A. Lee, A. Pooley, A. Gupta, A. Mandlekar, et al. Open x-embodiment: Robotic learning datasets and rt-x models. arXiv preprint arXiv:2310.08864, 2023.

OpenAI. Chatgpt: Optimizing language models for dialogue, 2023. URL https://openai.com/blog/chatgpt/.

OpenAI. Introducing chatgpt agent: bridging research and action, 2025a. URL https://openai.com/index/introducing-chatgpt-agent.

OpenAI. Introducing deep research, 2025b. URL https://openai.com/index/introducing-deep-research/.

openai. Operator, 2025. URL https://openai.com/index/introducing-operator/.

Y. Qin, Y. Ye, J. Fang, H. Wang, S. Liang, S. Tian, J. Zhang, J. Li, Y. Li, S. Huang, et al. Ui-tars: Pioneering automated gui interaction with native agents. arXiv preprint arXiv:2501.12326, 2025.

N. Ravi, V. Gabeur, Y.-T. Hu, R. Hu, C. Ryali, T. Ma, H. Khedr, R. Rädle, C. Rolland, L. Gustafson, et al. Sam 2: Segment anything in images and videos. arXiv preprint arXiv:2408.00714, 2024.

B. Seed. Ui-tars-1.5. https://seed-tars.com/1.5, 2025.

N. M. Shafiullah, Z. Cui, A. A. Altanzaya, and L. Pinto. Behavior transformers: Cloning k modes with one stone. Advances in neural information processing systems, 35:22955–22968, 2022.

Z. Shao, P. Wang, Q. Zhu, R. Xu, J. Song, X. Bi, H. Zhang, M. Zhang, Y. Li, Y. Wu, et al. Deepseekmath: Pushing the limits of mathematical reasoning in open language models. arXiv preprint arXiv:2402.03300, 2024.

L. Song, Y. Dai, V. Prabhu, J. Zhang, T. Shi, L. Li, J. Li, S. Savarese, Z. Chen, J. Zhao, R. Xu, and C. Xiong. Coact-1: Computer-using agents with coding as actions. arXiv preprint arXiv:2508.03923, Aug. 2025.

G. Team, R. Anil, S. Borgeaud, J.-B. Alayrac, J. Yu, R. Soricut, J. Schalkwyk, A. M. Dai, A. Hauth, K. Millican, et al. Gemini: a family of highly capable multimodal models. arXiv preprint arXiv:2312.11805, 2023.

S. T. Team. Ui-tars-2 technical report: Advancing gui agent with multi-turn reinforcement learning. arXiv preprint arXiv: 2509.02544, 2025.

H. Touvron, T. Lavril, G. Izacard, X. Martinet, M.-A. Lachaux, T. Lacroix, B. Rozière, N. Goyal, E. Hambro, F. Azhar, et al. Llama: Open and efficient foundation language models. arXiv preprint arXiv:2302.13971, 2023.

A. Van Den Oord, O. Vinyals, et al. Neural discrete representation learning. Advances in neural information processing systems, 30, 2017.

P. Wang, S. Bai, S. Tan, S. Wang, Z. Fan, J. Bai, K. Chen, X. Liu, J. Wang, W. Ge, et al. Qwen2-vl: Enhancing vision-language model's perception of the world at any resolution. arXiv preprint arXiv:2409.12191, 2024a.

Z. Wang, S. Cai, G. Chen, A. Liu, X. Ma, Y. Liang, and T. CraftJarvis. Describe, explain, plan and select: interactive planning with large language models enables open-world multi-task agents. In Proceedings of the 37th International Conference on Neural Information Processing Systems, pages 34153–34189, 2023.

Z. Wang, S. Cai, A. Liu, Y. Jin, J. Hou, B. Zhang, H. Lin, Z. He, Z. Zheng, Y. Yang, et al. Jarvis-1: Open-world multi-task agents with memory-augmented multimodal language models. IEEE Transactions on Pattern Analysis and Machine Intelligence, 2024b.

Z. Wang, S. Cai, Z. Mu, H. Lin, C. Zhang, X. Liu, Q. Li, A. Liu, X. Ma, and Y. Liang. Omnijarvis: Unified vision-language-action tokenization enables open-world instruction following agents. Advances in Neural Information Processing Systems, 2024c.

Z. Wang, A. Liu, H. Lin, J. Li, X. Ma, and Y. Liang. Rat: Retrieval augmented thoughts elicit context-aware reasoning in long-horizon generation. arXiv preprint arXiv:2403.05313, 2024d.

Z. Wang, M. Li, K. He, X. Wang, Z. Mu, A. Liu, and Y. Liang. Openha: A series of open-source hierarchical agentic models in minecraft. arXiv preprint arXiv:2509.13347, 2025a.

Z. Wang, X. Li, Y. Ye, J. Fang, H. Wang, L. Liu, S. Liang, J. Lu, Z. Wu, J. Feng, et al. Game-tars: Pretrained foundation models for scalable generalist multimodal game agents. arXiv preprint arXiv:2510.23691, 2025b.

Y. Xu, Z. Wang, J. Wang, D. Lu, T. Xie, A. Saha, D. Sahoo, T. Yu, and C. Xiong. Aguvis: Unified pure vision agents for autonomous gui interaction. arXiv preprint arXiv:2412.04454, 2024.

Y. Yan, S. Wang, J. Du, Y. Yang, Y. Shan, Q. Qiu, X. Jia, X. Wang, X. Yuan, X. Han, M. Qin, Y. Chen, C. Peng, S. Wang, and M. Xu. Mcp-world: A unified benchmarking testbed for api, gui, and hybrid computer use agents. arXiv preprint arXiv:2506.07672, 2025.

A. Yang, A. Li, B. Yang, B. Zhang, B. Hui, B. Zheng, B. Yu, C. Gao, C. Huang, C. Lv, et al. Qwen3 technical report. arXiv preprint arXiv:2505.09388, 2025.

J. Yang, C. E. Jimenez, A. Wettig, K. Lieret, S. Yao, K. Narasimhan, and O. Press. SWE-agent: Agent-computer interfaces enable automated software engineering. arXiv preprint arXiv:2405.15793, 2024.

H. Yuan, Z. Mu, F. Xie, and Z. Lu. Pre-training goal-based models for sample-efficient reinforcement learning. In The Twelfth International Conference on Learning Representations, 2024.

Y. Zhong, F. Bai, S. Cai, X. Huang, Z. Chen, X. Zhang, Y. Wang, S. Guo, T. Guan, K. N. Lui, et al. A survey on vision-language-action models: An action tokenization perspective. arXiv preprint arXiv:2507.01925, 2025a.

Y. Zhong, X. Huang, R. Li, C. Zhang, Y. Liang, Y. Yang, and Y. Chen. Dexgraspvla: A vision-language-action framework towards general dexterous grasping, 2025b.

A. Environment Details

In this work, we utilize Minecraft as the primary testbed for evaluating our agent's capabilities in multi-task reinforcement learning following large-scale pretraining. Minecraft provides a rich, dynamic environment that necessitates both embodied interactions (e.g., navigation, combat) and complex GUI-based operations (e.g., crafting, inventory management). This duality makes it an ideal benchmark for testing generalist agents capable of mastering diverse, open-ended tasks ranging from low-level motor control to high-level strategic planning.

A.1. Environment Configuration

Minecraft is an open-world sandbox game where players interact with and modify a procedurally generated 3D world. The game offers a vast array of tasks that resemble real-world challenges. Consequently, agents must navigate complex terrains, manage sparse rewards, and engage in long-horizon planning. Additionally, the game's popularity provides a wealth of potential training data, including gameplay videos and textual tutorials, making it invaluable for research into large-scale learning from unstructured data.

Our experimental setup follows the Variable Pretraining Task (VPT) protocol (Baker et al., 2022), where agents interact with the game in a manner identical to human players. Specifically, the **observation space** consists exclusively of raw RGB screenshots as visual input, with a resolution of 640×360, at a frequency of 20 Hz. No high-level or privileged state information (such as voxel grids or coordinate data) is provided during evaluation. Regarding **interaction modes**, the environment presents a dual challenge: while most observations consist of embodied first-person views, tasks such as crafting and smelting require the agent to operate within distinct GUI interfaces. As illustrated in Figure 7, the agent must seamlessly switch between handling continuous embodied interactions and discrete GUI-based operations.

A.2. Raw Action Space

The raw action space is designed to align with human interfaces, utilizing the native mouse and keyboard controls provided by MineRL v0.4 (Minecraft version 1.16.5) (Guss et al., 2019). A summary of the action mapping is provided in Table 3.

Mouse Control.. Mouse displacements are discretized into 1800 bins, and their semantic meaning is context-dependent. In **embodied mode**, these displacements control the camera orientation via pitch (Δy) and yaw (Δx) adjustments; in **GUI mode**, they correspond to 2D cursor movements on the screen. Mouse clicks are encoded as dedicated tokens representing left, right, and middle button presses.

Keyboard Control. Keyboard actions are treated as unique tokens, covering alphabetic characters (e.g., 'W', 'A', 'S', 'D' for movement), numeric digits (for hotbar selection), and special keys (e.g., `Shift`, `Space`, `Esc`).

A.3. Challenges for Reinforcement Learning

Minecraft presents several unique challenges that test the robustness and generalization capabilities of RL agents:

High Information Density. The environment is visually complex, featuring diverse textures, lighting conditions, and objects. Agents must efficiently process high-dimensional sensory inputs to identify relevant cues while filtering out irrelevant background noise. Specific challenges include distinguishing block types for crafting or spotting hostile mobs in low-light conditions. This requires strong visual representation learning and attention mechanisms.

Task Variety and Generalization. The open-ended nature of Minecraft offers a vast spectrum of tasks, ranging from primitive resource gathering to complex architectural construction. Agents must learn to generalize skills across these tasks. For instance, the motor skills required to chop a tree can be adapted to combat, while the logic used for crafting a wooden pickaxe serves as a foundational step for crafting diamond tools. This variety forces the agent to acquire adaptable,

Figure 7 | Representative observations in Minecraft, consisting of 640 × 360 RGB images. The agent must handle diverse visual contexts, including embodied first-person views (left) and GUI-based interfaces (right) for tasks like crafting and inventory management.

transferable strategies rather than memorizing fixed sequences.

Reward Sparsity. Unlike arcade games with frequent score updates, Minecraft rewards are often extremely sparse and delayed. For example, crafting a high-level item (e.g., a diamond sword) requires a long sequence of prerequisite actions: mining wood, crafting a crafting table, mining stone, smelting iron, and finding diamonds. The agent typically receives no feedback until the final goal is achieved. This necessitates efficient exploration strategies and the ability to reason over long horizons.

Dynamic Environment. The game features a dynamic world with day-night cycles, changing weather, and autonomous entities (mobs). An agent must adapt its decision-making to these variables—for example, seeking shelter at night to avoid monsters or navigating slippery terrain during rain. This dynamic nature ensures that agents are tested on their ability to adapt to non-stationary environments.

Table 3 | Summary of the human-aligned raw action space used by our agent. The agent interacts via standard keyboard and mouse inputs, identical to a human player.

Action Type	Human Input	Description
Movement	W	Move forward.
	S	Move backward.
	A	Strafe left.
	D	Strafe right.
	Space	Jump / Swim up.
	Left Shift	Sneak (prevents falling off edges).
	Left Ctrl	Sprint (increases movement speed).
Interaction	Left Mouse	Break blocks (hold) / Attack entities (click).
	Right Mouse	Place blocks / Interact with items / Open GUIs.
Inventory	Keys 1–9	Select corresponding hotbar slot.
Camera	Mouse X	Yaw: Horizontal rotation (−180° to 180°).
	Mouse Y	Pitch: Vertical rotation (−180° to 180°).

B. Action Spaces

In the context of Hierarchical Agents (HA), the design of the action space is pivotal, effectively dictating the agent's granularity of interaction with the environment. Existing approaches utilize varying levels of abstraction, spanning from atomic environmental controls to high-level semantic planning. The controllers associated with these spaces range in complexity from simple heuristic scripts to sophisticated Large Language Models (LLMs). Typically, as the level of abstraction increases, the reliability of execution becomes harder to guarantee, necessitating more robust decoders to bridge the gap between intent and execution.

Raw Actions represent the lowest level of the hierarchy. They directly link the agent to the environment's native interface by mimicking basic input devices, such as keyboards and mice (Kim et al., 2024; Zhong et al., 2025a).

Language Skills operate at a high level of abstraction, where the action space comprises goal-oriented commands expressed in natural language. These semantic instructions are interpreted by the agent's policy, which decodes them into sequences of lower-level primitives conditioned on the current visual observation (Driess et al., 2023; Wang et al., 2023).

Motion Actions serve as an intermediate abstraction, focusing on temporally extended, object-agnostic movement primitives. By encapsulating complex navigational or manipulation behaviors without binding them to specific object instances, they offer a more flexible representation com-

pared to step-by-step atomic actions (Belkhale et al., 2024b; Lifshitz et al., 2024).

Grounding Actions further enhance abstraction by explicitly incorporating spatial constraints. This paradigm enables the agent to target specific objects based on their coordinates in visual space. By decoupling the semantic intent of an action from its spatial execution parameters, grounding actions significantly improve generalization across diverse visual scenarios (Cai et al., 2024; Lee et al., 2025; Zhong et al., 2025b).

Latent Actions are derived via self-supervised learning rather than manual definition. Typically encoded into continuous embeddings and subsequently discretized into tokens, these actions allow the agent to operate within a learned abstract space. This approach eliminates the need for human-engineered heuristics, facilitating the acquisition of complex policies directly from large-scale offline data (Deng et al., 2025; Shafiullah et al., 2022; Van Den Oord et al., 2017; Yuan et al., 2024).

Collectively, these diverse action spaces contribute to the hierarchical structure of modern agents, providing a scalable and flexible framework for managing tasks of increasing complexity.

C. RL Algorithms

As detailed in section 3, our training framework incorporates two reinforcement learning phases: Single-Turn RL (STRL) and Multi-Turn RL (MTRL). Both phases utilize Group Relative Policy Optimization (GRPO) as the underlying optimization algorithm.

C.1. Single-Turn GRPO

Standard GRPO optimizes the policy by leveraging group-level statistics. The optimization objective follows the formulation defined in Equation 1 in section 3.

Unlike PPO, GRPO calculates the advantage $\hat{A}_i$ directly from the sampled group outputs without

a critic network:

$$\hat{A}_i = \frac{r_i - \text{mean}(\{r_1, \ldots, r_G\})}{\text{std}(\{r_1, \ldots, r_G\}) + \delta} \tag{7}$$

where r_i is the reward for the i-th output, and δ (e.g., 10^{-8}) is a small constant added for numerical stability.

The inclusion of the KL-divergence penalty term βD_{KL} acts as a regularizer, ensuring the updated policy does not deviate significantly from the reference model, thereby preventing reward hacking and maintaining linguistic coherence.

C.2. Multi-Turn GRPO

In the multi-turn setting, we adapt the single-turn formulation to handle sequential interactions. We decompose each trajectory τ into a set of state–response pairs and assign the final trajectory-level reward $r(\tau)$ to all intermediate responses.

Let $\mathcal{T}$ denote the trajectory space. The Multi-Turn GRPO objective is defined as:

$$J_{\text{MT}}(\theta) = \mathbb{E}_{\{\tau_i\}_{i=1}^G \sim \pi_{\text{old}}} \left\{ \frac{1}{G} \sum_{i=1}^{G} \frac{1}{L_i} \sum_{j=1}^{L_i} \frac{1}{|o_{i,j}|} \sum_{t=1}^{|o_{i,j}|} \left[\right.\right.$$

$$\min\left(\rho_{i,j,t}\hat{A}_i, \text{clip}\left(\rho_{i,j,t}, 1-\epsilon, 1+\epsilon\right)\hat{A}_i \right)$$

$$\left.\left. - \beta D_{\text{KL}}\left[\pi_\theta(\cdot|s_{i,j}) || \pi_{\text{ref}}(\cdot|s_{i,j})\right] \right] \right\} \tag{8}$$

where L_i is the number of turns in trajectory i, and the advantage $\hat{A}_i$ is computed using the group-relative statistics of the trajectory rewards $r(\tau_i)$. This allows the sparse, episodic reward to guide the optimization of every step in the trajectory.

D. Training Details

D.1. Base Model

To enable robust multi-modal reasoning and high-level planning, our system is built upon a pre-trained Vision-Language Model (VLM). Specifically, we initialize our system with the open-source **OpenHA** model Wang et al. (2025a), which is derived from Qwen2-VL-7B Wang et al.

(2024a). We selected this model for its demonstrated proficiency in Minecraft-specific visual grounding and its strong instruction-following capabilities within the domain.

D.2. Training Implementation

As detailed in section 3, our training pipeline comprises three progressive stages: Cold-Start Supervised Fine-Tuning (SFT), Single-Turn Reinforcement Learning (STRL), and Multi-Turn Reinforcement Learning (MTRL). To ensure experimental consistency and reproducibility, all models were trained on a cluster of 8 NVIDIA A800-SXM4-80GB GPUs, using Python 3.10 and CUDA 12.6.

The specific hyperparameter configurations for each stage are summarized in Table 4. We maintain consistent hyperparameter settings for the SFT process across both the initial Stage 1 and the cold-start phases to isolate the impact of training data and objectives

Table 4 | Hyperparameter settings across different training stages.

Hyperparameter	SFT	STRL	MTRL
Total Training Tokens	0.07B	0.14B	1.41B
Training Samples (Images)	12K	24K	1.3M
Trainable Components	Full	Full	Full
Global Batch Size	512	1272	128
Optimizer	AdamW	AdamW	AdamW
LR Warmup Steps	15	0	0
Maximum Learning Rate	8.0×10^{-6}	1.0×10^{-6}	5.0×10^{-6}
Minimum Learning Rate	1.0×10^{-6}	1.0×10^{-6}	5.0×10^{-6}
Group Size (G)	-	4	4
KL Coefficient (β)	-	0.01	0.01
Clipping Parameter (ϵ)	-	0.2	0.2